

LogICL: Distilling LLM Reasoning to Bridge the Semantic Gap in Cross-Domain Log Anomaly Detection

Jingwei Ye, Zhi Wang, Chenbin Su, Jieshuai Yang, Jiayi Ding, Chunbo Liu, and Ge Chu, *Member, IEEE*

Abstract—Effective log anomaly detection is critical to sustaining reliability in large-scale IT infrastructures. Transformer-based language models have advanced the field but require substantial computational resources and labeled data, exacerbating the cold-start problem in target domains where logs are scarce due to system evolution. Cross-domain methods alleviate data scarcity by leveraging source domain logs. However, their reliance on surface lexical similarity limits cross-domain generalization, as they fail to capture latent semantic equivalence amid structural and terminological divergences.

To address these challenges, we propose LogICL, a framework that distills Large Language Model (LLM) reasoning into a lightweight encoder for cross-domain anomaly detection. During training, LogICL constructs a delta matrix by measuring the utility of demonstrations selected via Maximal Marginal Relevance algorithm relative to zero-shot inference. The encoder is jointly optimized via a multi-objective loss comprising an ICL-Guided term that pulls together representations of source-target pairs with positive reasoning assistance while pushing apart interfering pairs in the representation space, maximum mean discrepancy for domain alignment, and supervised contrastive loss for anomaly discrimination. At inference, the optimized encoder retrieves reasoning-aware demonstrations based on semantic similarity and delta scores, enabling frozen-LLM in-context learning with chain-of-thought reasoning for accurate and interpretable anomaly detection.

Experiments on few-shot and zero-shot cross-domain benchmarks confirm that LogICL achieves state-of-the-art performance across heterogeneous log systems. Further experimental validation via alignment visualizations and case studies confirms that LogICL bridges the semantic gap beyond surface lexical similarity, effectively capturing latent semantic equivalence for rapid deployment in new systems.

Index Terms—Log anomaly detection, Cross domain, In-context learning, Latent semantic equivalence, Large language model.

I. INTRODUCTION

Modern large-scale software systems—including distributed platforms, cloud services, and enterprise infrastructures—produce massive volumes of logs that capture system operations, component interactions, and runtime states. As a

(Corresponding author: Zhi Wang.)

Jingwei Ye, Zhi Wang, Chenbin Su, Jieshuai Yang are with the College of Cryptology and Cyber Science, Nankai University, Tianjin 300350, China (e-mail: jwye@mail.nankai.edu.cn; zwang@nankai.edu.cn; champion.su@mail.nankai.edu.cn; yjs@mail.nankai.edu.cn).

Jiayi Ding is with the School of Computer Science and Artificial Intelligence, Civil Aviation University of China, Tianjin 300300, China (e-mail: 221240005@cauc.edu.cn)

Chunbo Liu is with the Information Security Evaluation Center, Civil Aviation University of China, Tianjin 300300, China (e-mail: luchamber@163.com)

Ge Chu is with the Research Department, Runjian Co., Ltd., Nanning 530200, China (e-mail: gechu@runjian.com)

primary source of observability, these logs are instrumental for maintaining system reliability and play a central role in diagnosing performance degradation, identifying service failures, and detecting anomalies. Consequently, effective log analysis is essential for ensuring the robustness and trustworthiness of modern computing systems.

Log-based anomaly detection has therefore become an indispensable technique for maintaining stable and dependable software operations, enabling timely identification and diagnosis of abnormal behaviors before they escalate into severe system disruptions [1], [2].

In recent years, Transformer-based language models have established a new paradigm in log anomaly detection, broadly categorized into Language Models (LMs) and Large Language Models (LLMs). LM-based approaches (e.g., LogBERT [3], NeuralLog [4], LogOW [5]) leverage masked language modeling and contextual embeddings to capture stable token-level patterns, enabling robust anomaly scoring with modest supervision. More recently, LLM-based methods (e.g., LogGPT [6], LogLLM [7]) have demonstrated remarkable capabilities in reasoning and few-shot generalization, utilizing high-capacity encoders and extensive pre-training to model complex, long-range log dependencies across diverse formats.

However, the superior performance of Transformer-based architectures comes at a significant cost. These models are data-intensive and computationally demanding, necessitating extensive labeled datasets for effective pre-training or fine-tuning. This dependency creates a fundamental conflict with the rapid evolution of modern software systems, where continuous updates lead to a scarcity of labeled logs in newly deployed environments [5], [8]. Consequently, the substantial parameter scale and training overhead render these models practical infeasible in data-scarce target domains.

To address data scarcity, cross-system methods attempt to transfer knowledge from high-resource source domains to target domains. LogTransfer [9] utilizes shared layers with Glove embeddings; LogTAD [10] employs adversarial domain adaptation technique training for cross domain; and Meta-Log [11] applies meta-learning to construct shared semantic spaces.

Despite existing methods have achieved preliminary success in mitigating data scarcity, they continue to face significant challenges in cross-domain scenarios. These challenges can be summarized in two key areas:

a) Surface Similarity vs. Latent Equivalence: Existing cross-domain log anomaly detection methods predominantly leverage static pre-trained word embeddings (e.g., GloVe [12])

to obtain semantic vector representations. While effective for logs with high lexical overlap, these approaches capture only *surface lexical similarity*, failing to model the *latent semantic equivalence* required for heterogeneous systems.

The upper part of Figure 1 demonstrates a scenario where static embeddings succeed due to substantial consistency. From the perspective of **syntactic structure**, both the Thunderbird (source domain) and BGL (target domain) logs adhere to a unified *Component-State-Reason* template. The source initiates with a kernel component (“modprobe”) followed by a severity level (“FATAL”), while the target begins with a component header (“ciod”) followed by an action state (“LOGIN ... failed”), and both conclude with the identical error reason (“No such file or directory”). In terms of **lexical vocabulary**, the two domains exhibit high overlap, sharing nearly identical error descriptors (e.g., the exact POSIX error “No such file or directory”). This structural and lexical alignment allows traditional methods to easily extract correlated features and facilitate positive transfer.

In contrast, the lower part of Figure 1 highlights the limitation of existing methods in identifying an identical *Network Transmission Failure*. From the perspective of **syntactic structure**, the domains show fundamental divergence. The Thunderbird (source domain) log adopts a *procedural narrative* typical of Java exceptions, detailing a specific action flow (“Failed to transfer blk_...” culminating in “java.io.IOException”). Conversely, the HDFS (target domain) log employs a *declarative key-value* format, listing component attributes (“sendmail”, “mailer=relay”) and status indicators (“stat=Deferred”). In terms of **lexical vocabulary**, the descriptions rely on disjoint terminology to convey the same meaning (“transfer/reset” vs. “relay/refused”). This significant discrepancy in both structure and vocabulary causes static embeddings to maximize the distance between these semantically equivalent vectors, leading to negative transfer.

b) *High Computational and Data Constraints of Language Models*: While Transformer-based models offer superior performance, their deployment is hindered by excessive resource demands. This constraint applies not only to massive LLMs but also to BERT-based LMs, which still require significant computational power for fine-tuning and inference compared to traditional methods. The dependence on high-quality labeled datasets further complicates their application in real-world environments where data is noisy or scarce. Even with efficient tuning strategies (e.g., LoRA [13]), the fundamental trade-off between model capacity and resource efficiency remains a persistent hurdle for scalable log analysis.

In summary, to address the aforementioned limitations, we propose LogICL, a novel framework that harnesses ICL to enhance cross-domain generalization and detection accuracy in few-shot log anomaly detection settings with scarce target-domain supervision. Specifically, LogICL tackles two key challenges: (1) the inadequate modeling of latent semantic equivalence across heterogeneous logs with varying structures and terminology; and (2) the substantial computational and data requirements of LMs, which often rely on resource-intensive training paradigms and abundant labeled data. The main contributions of this paper can be summarized as follows:

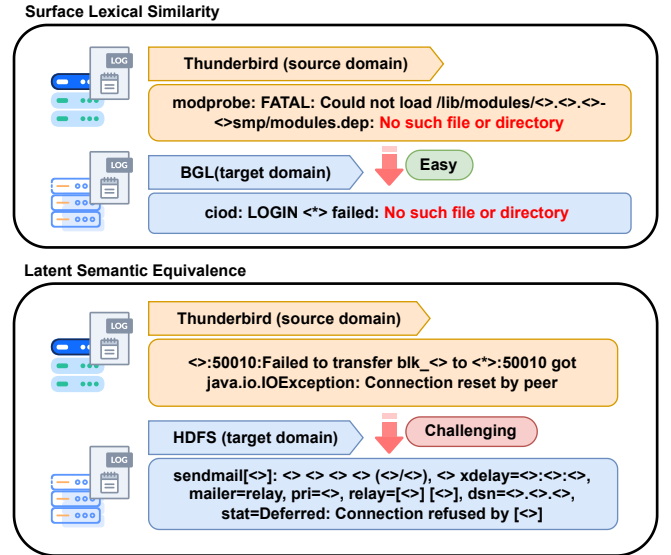


Fig. 1. Surface Lexical Similarity & Latent Semantic Equivalence.

- We propose LogICL, a novel log anomaly detection framework that integrates ICL as a key component. It introduces a reasoning-guided, representation-aware demonstration selection paradigm that leverages LLM reasoning feedback to refine the encoder and identify demonstrations most beneficial for downstream inference. This mechanism enables the model to generalize effectively under data-scarce target domains without requiring updates to LLM parameters, allowing LogICL to surpass existing log anomaly detection methods in both few-shot and zero-shot scenarios.
- We propose LogICL, which enhances cross-domain knowledge transfer by leveraging the causal reasoning capabilities of large models. It aligns logs describing similar events with different phrasing and structures, extracting shared knowledge across domains. This enables more accurate anomaly detection in heterogeneous environments, facilitating robust log analysis across diverse systems and improving detection performance.

II. PRELIMINARIES AND RELATED WORK

A. Preliminaries

Transfer Learning (TL) constitutes a machine learning paradigm designed to improve generalization in a target domain by leveraging knowledge acquired from related source domains [14], [15]. Fundamentally, TL relaxes the independent and identically distributed (i.i.d.) assumption inherent in traditional supervised learning, enabling effective model adaptation across domains with shifting distributions or disparate feature spaces, particularly under supervision scarcity [16]. Existing methodologies are generally categorized into three paradigms: (1) instance-based approaches, which mitigate distribution mismatch (e.g., covariate shift) by reweighting or selecting source samples that structurally resemble target instances; (2) feature-based approaches, which project source and target data into a shared, domain-invariant latent space to align marginal

or conditional distributions; and (3) model-based approaches, which transfer structural knowledge or inductive biases by reusing pre-trained parameters and architectures to accelerate downstream adaptation.

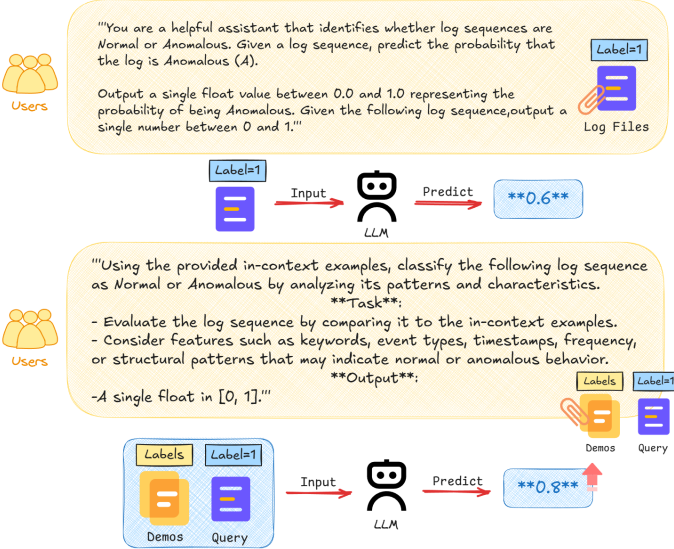


Fig. 2. In-context learning example for log anomaly detection.

The advent of LLMs has popularized In-Context Learning (ICL), a paradigm that enables models to adapt to downstream tasks without parameter updates [17], [18]. In this setting, the model is conditioned on a few task-specific demonstrations prepended to the input query. By attending to these contextual examples, LLMs can infer the task intent and generate desired outputs, leveraging analogies within the context window to achieve few-shot generalization [19]. In contrast to gradient-based fine-tuning, ICL relies on inference-time prompting, where the model’s output is strongly influenced by the choice, sequence, and presentation of these demonstrations [20]. From a theoretical perspective, this process can be interpreted as implicit Bayesian inference or meta-optimization mediated by the model’s attention mechanisms [21], [22]. As a result, ICL enables strong few-shot generalization, effectively linking pre-training knowledge to downstream applications in data-constrained environments.

Fig. 2 demonstrates the effectiveness of ICL for log analysis. While standard prompting often yields suboptimal performance on complex log patterns, ICL enhances the results by introducing reference examples. As illustrated, when an LLM analyzes a log query directly, the detection accuracy is often limited. To address this, relevant samples are selected to serve as in-context demonstrations. By providing these demonstrations alongside the query, the LLM utilizes the context to output a more accurate prediction.

B. Related Work

The traditional log anomaly detection pipeline, as illustrated in Fig. 3, typically consists of six stages: (1) log collection (2) preprocessing raw log messages to remove erroneous identifiers and incomplete logs; (3) log parsing to convert

unstructured text into structured event templates; (4) log grouping to form context-aware sequences (e.g., by session or time); (5) feature extraction to transform textual data into vector representations; and (6) anomaly detection by training learning-based models on these vectors to identify anomalies.

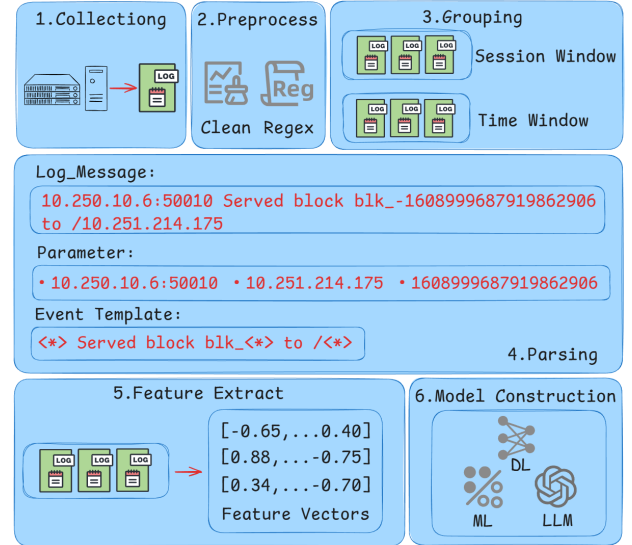


Fig. 3. Traditional workflow of log anomaly detection.

In recent years, LLMs have attracted growing interest in log anomaly detection. In the log parsing stage, approaches such as LLMParse [23], LogPrompt, and LogRules [24] leverage LLMs—either through fine-tuning or prompting—to extract structured event templates from raw log messages. In the anomaly detection stage, existing methods can be broadly classified into two categories: parameter-freezing and parameter-tuning approaches. Parameter-freezing methods, including FlexLog [25], LogPrompt, LogRules, EagerLog [26], and LogRAG, rely on the generalization ability of pretrained LLMs while keeping all model parameters frozen. In contrast, parameter-tuning (fine-tuning-based) methods—such as LogGPT [6], LogLLM [7], SuperLog [27], NLPLLog [27], and RationAnomaly [28]—adapt LLMs to log-specific tasks by updating model parameters.

Our work addresses the cold-start scenario characterized by scarce source domain data and the resulting semantic gap. By retrieving optimal demonstrations to facilitate ICL with a frozen LLM, our framework bridges the cross-domain gap without parameter optimization. This strategy efficiently harnesses the model’s generalization capabilities for zero-shot and few-shot anomaly detection.

III. DESIGN OF MODEL

A. Overview

As illustrated in Figure 4, LogICL is a framework designed to distill the reasoning capabilities of LLMs into a log sequence encoder for effective cross-domain anomaly detection. The workflow operates in two phases: training and inference(test). During the training phase (left panel), we

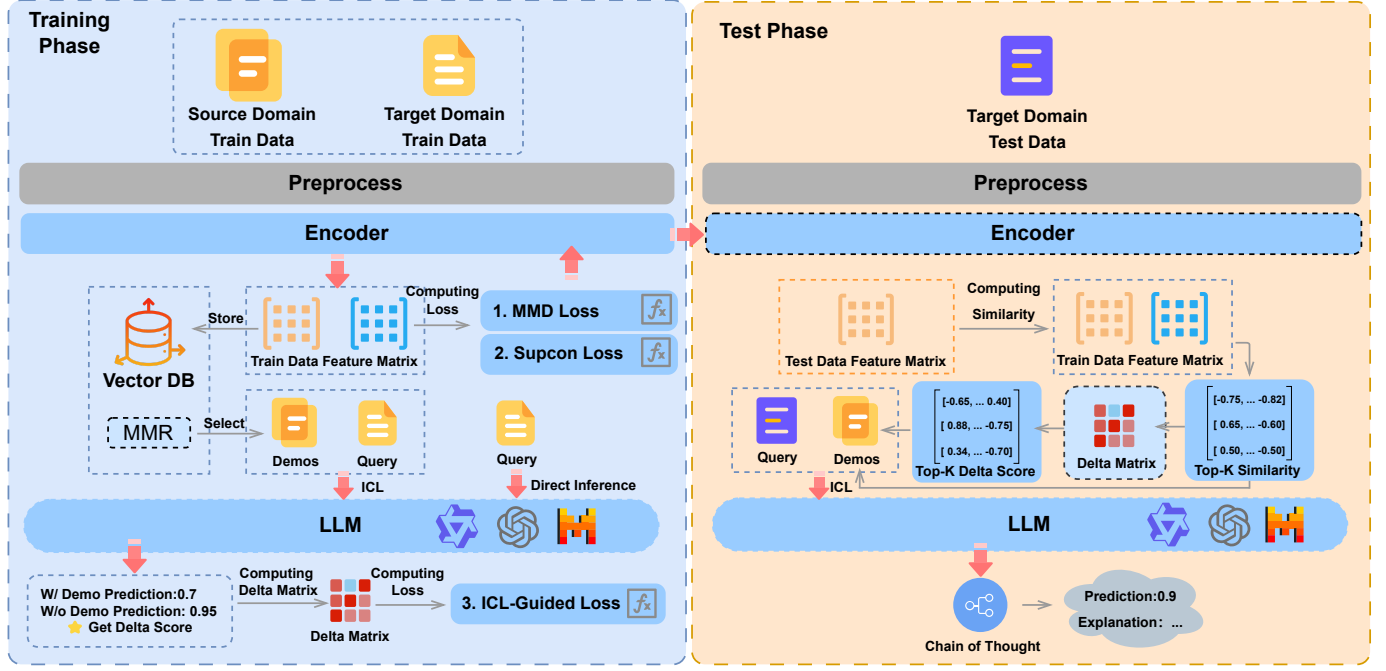


Fig. 4. Overall framework of LogICL.

first construct a sparse delta matrix by evaluating the zero-shot and one-shot performance of an LLM using demonstrations selected via Maximal Marginal Relevance (MMR) [29]. This matrix systematically quantifies the directional utility of training samples, providing a robust supervision signal that guides the encoder optimization through a novel ICL-Guided Loss. To ensure comprehensive representation learning, the encoder is jointly optimized using a multi-objective function that integrates the ICL-Guided Loss with Maximum Mean Discrepancy (MMD) Loss for domain alignment and Supervised Contrastive (SupCon) Loss for anomaly discrimination. In the inference phase (right panel), LogICL leverages this optimized encoder to retrieve demonstrations based on a hybrid metric of semantic similarity and learned delta utility. These high-quality demonstrations are then fed into the LLM to perform interpretable, Chain-of-Thought (CoT) enhanced anomaly detection on target domain data.

B. Pre-processing

Traditional log analysis employs parsers (e.g., Drain [30]) to split raw log messages into constant *event templates* and dynamic *parameters*, as illustrated in Fig. 3. However, this parsing process introduces inherent limitations. First, parsing algorithms may misidentify variable parameters as template tokens. This error generates fragmented templates for logs belonging to the same event category, artificially introducing “unseen formats” that inject noise into downstream detection tasks [4], [31]–[33]. Second, discarding dynamic parameters results in the loss of semantic information that is valuable for detection accuracy. Recent studies indicate that Transformer-based models can achieve robust performance directly on raw log text without explicit parsing [4], [7].

Consequently, we adopt a **parser-free strategy**. We utilize regular expressions for basic preprocessing, which avoids parsing-induced noise while preserving raw parameter details (e.g., IP addresses, *block_id*). Crucially, retaining these parameters enables the downstream LLM to leverage the full semantic context during inference, thereby enhancing detection accuracy and providing interpretable diagnostics that help operation experts narrow the scope of anomaly localization.

C. Log Sequences Representation Learning

Following preprocessing, raw log messages are grouped into sequences to capture system execution flows. This is achieved via two strategies: session-based partitioning, which aggregates messages by identifiers (e.g., *block_id* in HDFS), and window-based partitioning (fixed or sliding) for continuous streams. This structuring is critical as it enables the model to detect anomalies based on sequential dependencies and behavioral patterns, rather than analyzing isolated log entries.

Let a log sequence be denoted as $s = \{m_1, m_2, \dots, m_L\}$, where s is a sequence of log messages m_i , and L is the sequence length. A training dataset of sequences is defined as $\mathcal{D}_{\text{train}} = \{s_1, s_2, \dots, s_N\}$, $s_i \in \mathcal{D}_{\text{train}}$, where N is the number of sequences in the training dataset. Each log sequence s_i is encoded into a fixed-dimensional embedding vector via the encoder f_e :

$$v_i = f_e(s_i) \in \mathbb{R}^d, \quad i = 1, \dots, N, \quad (1)$$

where v_i denotes the embedding vector of sequence s_i and d is the embedding dimension (i.e., the number of features representing each sequence).

Collectively, the set of embeddings for the training dataset is

$$\mathcal{E} = \{v_1, v_2, \dots, v_N\} \subset \mathbb{R}^d, \quad (2)$$

where \mathcal{E} represents the embedding space of all training sequences.

In cross-domain log anomaly detection, robust representation learning hinges on extracting domain-invariant features. Ideally, the encoder should suppress irrelevant system-specific variations via domain alignment to facilitate transfer. However, an inherent tension exists: aggressive alignment can precipitate negative transfer by erasing task-critical semantics. Since anomalies in heterogeneous systems often manifest through distinct keywords (e.g., *block lost* in HDFS vs. *file system full* in BGL), indiscriminate alignment risks treating these discriminative features as domain noise. Therefore, an effective framework must navigate this trade-off, bridging the distributional gap while rigorously preserving the semantic discriminability of system-specific anomalies.

D. Training Phase

The training phase of LogICL is composed of two primary stages. First, we construct a delta matrix via ICL on the training set. This matrix quantifies the extent to which a specific demonstration log sequence contributes to the correct inference of a query sequence. Second, we optimize the log sequence encoder using a Multi-Objective Loss Function that integrates ICL-Guided Loss.

1) *Construction of Delta Matrix*: We construct a delta matrix to systematically quantify the extent to which a specific training sample, acting as a demonstration, enhances the inference accuracy of a target query sequence. Let $\mathcal{S}_{train} = \{s_1, \dots, s_N\}$ denote the training set, where each sequence s_q serves as both a potential query and a demonstration candidate. The construction process involves two steps: demonstrations selection via MMR and influence quantification via delta scores.

a) *Demonstrations Selection*: Exhaustively computing delta scores for all pairwise combinations in the training set \mathcal{S}_{train} entails performing LLM inference $O(N^2)$ times, which is computationally prohibitive. To circumvent this overhead, we prune the search space for each query sequence s_q (with embedding \mathbf{q}) by retrieving a dedicated *demonstration set* \mathcal{D}_q of size k . Instead of relying solely on cosine similarity—which often yields redundant samples—we employ the MMR algorithm to balance semantic *relevance* with *diversity* [34].

Formally, we iteratively construct the demonstration set \mathcal{D}_q by selecting samples from the available training pool \mathcal{S}_{train} . Let S denote the subset of demonstrations selected in previous iterations (initialized as $S = \emptyset$). In each step, MMR identifies the optimal sample s^* (with embedding \mathbf{d}^*) that maximizes the following marginal relevance objective:

$$s^* = \arg \max_{s_j \in \mathcal{S}_{train} \setminus S} \left[\underbrace{\lambda \cdot \text{sim}(\mathbf{q}, \mathbf{d}_j)}_{\text{Relevance}} - \underbrace{(1 - \lambda) \cdot \max_{s_k \in S} \text{sim}(\mathbf{d}_j, \mathbf{d}_k)}_{\text{Diversity Penalty}} \right] \quad (3)$$

where \mathbf{q} and \mathbf{d}_j represent the embeddings of the query log s_q and a candidate sample s_j , respectively. The hyperparameter $\lambda \in [0, 1]$ balances the trade-off between relevance to the query and diversity within the selected set. Specifically, the first term

encourages selecting samples semantically close to the query, while the second term penalizes candidates that are too similar to already selected demonstrations ($s_k \in S$), thereby reducing redundancy. The selected s^* is added to S until the budget $|S| = k$ is met, at which point $\mathcal{D}_q \leftarrow S$.

b) *Computation of Delta Scores*: After retrieving the demonstration set \mathcal{D}_q for each query s_q , we systematically quantify the contribution of each demonstration $s_d \in \mathcal{D}_q$. We define the delta score, $\delta(s_q, s_d)$, as the reduction in absolute prediction error achieved by conditioning the inference on s_d .

Let $l(s_q) \in \{0, 1\}$ denote the ground truth label. We define the prediction error in the zero-shot setting as $e_{\text{zero}}(s_q) = |p_0(s_q) - l(s_q)|$, and in the one-shot setting as $e_{\text{one}}(s_q, s_d) = |p_1(s_q | s_d) - l(s_q)|$, where p_0 and p_1 represent the anomaly probabilities predicted by the LLM in the absence and presence of the demonstration s_d , respectively. The delta score is formulated as:

$$\delta(s_q, s_d) = e_{\text{zero}}(s_q) - e_{\text{one}}(s_q, s_d) \quad (4)$$

A positive δ indicates that s_d provides informative context that aligns the prediction with the true label, whereas a negative value suggests the introduction of noise.

Finally, we aggregate these scores into a sparse matrix $\mathbf{M}_\delta \in \mathbb{R}^{N \times N}$. The entry corresponding to query s_q and demonstration s_d is defined as:

$$(\mathbf{M}_\delta)_{qd} = \begin{cases} \delta(s_q, s_d) & \text{if } s_d \in \mathcal{D}_q \\ 0 & \text{otherwise} \end{cases} \quad (5)$$

This selective computation restricts the complexity to $O(N \cdot k)$, effectively filtering out irrelevant pairs while providing a robust supervision signal for the subsequent encoder optimization.

2) *Multi-Objective Loss Function*: We design a multi-objective loss function to jointly optimize the encoder, which comprises three components: (1) Domain Alignment Loss, (2) Task-Specific Loss and (3) ICL-Guided Loss.

a) *Domain Alignment Loss*: To mitigate the discrepancy between source and target domains, we introduce a Domain Alignment Loss that enforces similarity between their latent feature distributions. The objective is to learn domain-invariant representations, such that feature embeddings from the source and target domains become indistinguishable in a shared latent space, thereby facilitating more effective cross-domain demonstration selection during ICL inference. This alignment is realized by minimizing the distributional discrepancy between the two domains through the Maximum Mean Discrepancy (MMD) criterion [29]. Specifically, MMD quantifies the distance between the feature embeddings of log sequences from the source and target domains in a Reproducing Kernel Hilbert Space (RKHS) [35]. By reducing this distance, the encoder learns to produce domain-invariant embeddings that capture task-relevant semantics while suppressing domain-specific biases, thus promoting more consistent and transferable reasoning across domains.

$$L_{\text{MMD}} = \left\| \frac{1}{N_h} \sum_{i=1}^{N_h} \phi(\text{Encoder}(s_{h_i})) - \frac{1}{N_b} \sum_{j=1}^{N_b} \phi(\text{Encoder}(s_{b_j})) \right\|_H \quad (6)$$

where ϕ is a Gaussian kernel, N_h and N_b are batch sizes for each domain, and H is the RKHS. This ensures embeddings are domain-consistent, facilitating source-to-target transfer in few-shot settings.

b) Task-Specific Loss: To enhance the discriminative capacity of the encoder, We employ a Supervised Contrastive Loss that encourages positive log sequence pairs (with the same label) to have closer embeddings in the representation space, while increasing the distance between negative pairs (log sequences with different labels) [36]. By leveraging label information, this loss explicitly strengthens intra-class cohesion and inter-class separation, leading to more structured and semantically consistent feature representations. Such discriminative embeddings provide a stronger foundation for downstream anomaly detection task:

$$L_{\text{SupCon}} = \frac{1}{B} \sum_{b=1}^B \sum_{i \in I_b} \frac{-1}{|P(i)|} \sum_{p \in P(i)} \log \left(\frac{\exp(s_{i,p}/\tau) + \epsilon}{\sum_{a \in A(i)} \exp(s_{i,a}/\tau) + \epsilon} \right) \quad (7)$$

where B denotes the batch size, $v_i = f_\theta(s_i) \in \mathbb{R}^d$ is the embedding vector of log sequence s_i encoded via the encoder f_θ , $P(i)$ denotes the set of positive log sequences sharing the same label as s_i , $A(i)$ is the set of all log sequences in the batch, $s_{i,p} = \text{sim}(v_i, v_p)$ for $v_p \in P(i)$ forming a positive pair with v_i , and $s_{i,a} = \text{sim}(v_i, v_a)$ for $v_a \in A(i)$.

c) ICL-Guided Loss: We introduce an ICL-Guided Loss based on the sparse delta matrix \mathbf{M}_δ to align the log sequence encoder with the LLM's inference behavior. This objective optimizes the embedding space to ensure retrieval selects demonstrations that improve prediction performance. As illustrated in Figure 5, after constructing delta matrix, the loss explicitly regulates vector distances based on ICL utility: the model pulls queries closer to demonstrations with positive delta scores, and pushes away those with negative scores. By utilizing sparse delta matrix \mathbf{M}_δ , the optimization processes only validated, informative pairs, ensuring efficient knowledge transfer without introducing noise from irrelevant sample combinations. The loss function consists of the following two components:

- The loss function for positive pairs (D^+) is formulated to increase the similarity between sample pairs to improve ICL inference accuracy.

$$L_{\text{Delta+}} = - \sum_{(i,j) \in D^+} \delta(s_q, s_d) \cdot \log \left(\frac{s_{i,j}}{\tau} \right) \quad (8)$$

where D^+ denotes the set of positive log sequence pairs, $\delta(s_q, s_d)$ is the delta score between query log sequence s_q and demonstration s_d , and $s_{i,j} = \text{sim}(v_i, v_j)$ denotes the cosine similarity between the embeddings of s_i and s_j , with τ as the temperature scaling factor.

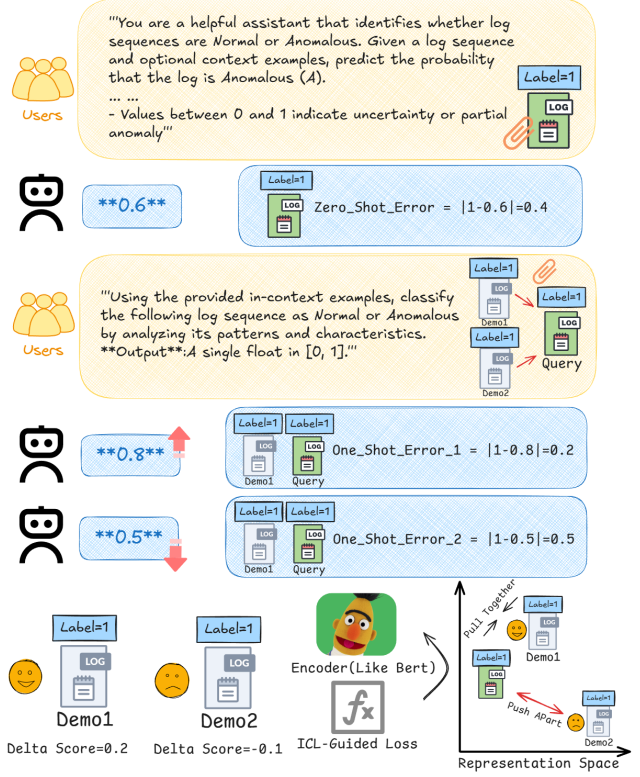


Fig. 5. Illustration of ICL-Guided Loss.

- The loss function for negative pairs (D^-) is formulated to reduce the embedding similarity between them.

$$L_{\text{Delta-}} = \sum_{(i,j) \in D^-} \max(0, |\delta(s_q, s_d)| - \theta) \cdot (1 - s_{i,j}) \quad (9)$$

The complete loss function is formulated as follows:

$$L_{\text{Delta}} = L_{\text{Delta+}} + \lambda_{\text{Delta-}} \cdot L_{\text{Delta-}} \quad (10)$$

where $\lambda_{\text{Delta-}}$ handles negative deltas by ignoring small interferences, balancing ICL guidance with domain consistency. Combining the above three types of loss functions, the overall Multi-Objective Loss Function L_{Multi} is formulated as follows:

$$L_{\text{Multi}} = \lambda_{\text{MMD}} \cdot L_{\text{MMD}} + \lambda_{\text{SupCon}} \cdot L_{\text{SupCon}} + \lambda_{\text{Delta}} \cdot L_{\text{Delta}} \quad (11)$$

where λ_{MMD} , λ_{SupCon} , and λ_{Delta} are hyperparameters controlling the relative importance of the domain alignment, task-specific, and ICL-Guided losses, respectively.

E. Test Phase

During inference, we employ a *Dual-Source Retrieval Strategy* to construct optimal in-context demonstrations. For a given test log s_t , encoded as $v_t = f'_{\text{encoder}}(s_t)$, the selection process proceeds in two stages to balance surface lexical similarity and latent semantic equivalence:

1) Similarity-based Anchoring: We first retrieve the $top-i$ nearest neighbors from the training set $\mathcal{D}_{\text{train}}$ based on cosine similarity to s_t . These samples form the similarity-based anchor set \mathcal{C}_{sim} :

$$\mathcal{C}_{\text{sim}} = \max_{s_j \in \mathcal{D}_{\text{train}}} \left(\frac{v_t \cdot v_j}{\|v_t\| \|v_j\|} \right) \quad (12)$$

2) *Delta-guided Expansion*: We leverage the retrieved anchors in \mathcal{C}_{sim} to query the pre-computed delta matrix. The underlying assumption is that optimal demonstrations for the anchors are likely effective for the test sample due to their high similarity. Specifically, we select the $top-j$ training samples that yielded the highest delta scores for the anchors in \mathcal{C}_{sim} . We aggregate these pre-computed scores and select the $top-j$ samples to form the expansion set \mathcal{C}_{delta} :

$$\mathcal{C}_{delta} = \underset{s_n \in \mathcal{D}_{train}}{top-j} \left(\sum_{s_m \in \mathcal{C}_{sim}} \delta_{m,n} \right) \quad (13)$$

where $\delta_{m,n}$ represents the pre-computed delta score of using s_n as a demonstration for anchor s_m . Finally, the LLM performs anomaly detection using the combined context $\mathcal{C}_{final} = \mathcal{C}_{sim} \cup \mathcal{C}_{delta}$.

3) *In-context and CoT Prediction*: The set $\mathcal{C}_{final} = \{s_1, s_2, \dots, s_k\}$ is selected to assist the LLM in performing inference on the test log s_t , where $\{y_1, y_2, \dots, y_k\}$ denote the corresponding labels.

$$\mathcal{P}_t = \{(s_1, y_1), (s_2, y_2), \dots, (s_k, y_k), s_t\}. \quad (14)$$

The prompt \mathcal{P}_t is then provided to the LLM to estimate the anomaly probability of the test log s_t :

$$p_t = LLM(\mathcal{P}_t), \quad (15)$$

where $p_t \in [0, 1]$ denotes the probability that s_t is anomalous. When CoT reasoning is enabled, the model provides a step-by-step diagnostic explanation before outputting p_t .

IV. EVALUATION

A. Experimental Design

1) *Datasets*: We evaluate our method on four public log benchmarks: HDFS, BGL, Thunderbird, and Liberty. These datasets encompass diverse system architectures and data distributions, providing a comprehensive testbed to evaluate the model's generalization capabilities. [37].

Distributed File System Logs: Represented by HDFS, this dataset is collected from 200 Amazon EC2 nodes and contains 11.18 million messages with a 2.93% anomaly ratio [38].

Supercomputing System Logs: This category includes BGL, Thunderbird, and Liberty, which are derived from high-performance computing environments but exhibit distinct alert characteristics. BGL is dominated by hardware alerts (98.04%) with a 7.34% anomaly ratio. In contrast, Thunderbird and Liberty primarily feature software-related alerts. Notably, Liberty presents a challenge of extreme imbalance with scarce anomalies, whereas Thunderbird contains a complex mix of uncertainty alerts [37].

2) *Data Preprocessing and Sampling*: We adopt distinct log grouping strategies based on the dataset structure. For HDFS, log messages are grouped by their unique *block_id*. For supercomputing datasets (BGL, Thunderbird, and Liberty), we employ fixed sliding windows (non-overlapping), setting the window size to 40 for BGL and Thunderbird, and 30 for Liberty. To prevent data leakage, we partition the training and testing sets strictly in chronological order. The resulting training dataset consists of 50,000 source domain sequences and only 5,000 target domain sequences.

TABLE I
DETAILS OF THE DATASETS

Dataset	Log Messages	Log Seq	Anomaly Log Seq
HDFS	11,175,629	575,061	16,838
BGL	4,713,520	117,838	24,697
Thunderbird	20,000,000	500,000	24,697
Liberty	5,000,000	166,667	110,427

3) *Cross-domain Evaluation Settings*: To evaluate the generalization capability of LogICL across HDFS, BGL, Thunderbird (TB), and Liberty, we design two settings with strictly defined data splits: (1) few-shot transfer: Simulating limited target supervision, the training set combines 50,000 source samples with 5,000 target samples. As shown in Table II (e.g., Liberty-BGL). During inference, $k = 8$ demonstrations are retrieved specifically from the training set to predict the test data. (2) zero-shot transfer: To assess robustness on unseen domains, the training set combines 50,000 primary source domain samples with 5,000 auxiliary source domain samples. As shown in Table III (e.g., the BGL-Liberty-TB), the model retrieves $k = 8$ demonstrations from primary source samples (BGL) and auxiliary source domain samples (Liberty) to predict unseen target domain samples (TB).

4) *Baselines*: To comprehensively evaluate the effectiveness of LogICL, we benchmark it against nine representative baselines across three major paradigms:

Deep Learning-based Approaches: We include LogRobust [39] as a standard supervised baseline. This method transforms distinct log events into semantic vectors and employs a Long Short-Term Memory (LSTM) network to capture temporal patterns and contextual semantics, enabling stable anomaly detection across variable log data.

Cross-System Approach: For cross-system scenarios, we adopt LogTransfer [9], LogTAD [10] and MetaLog [11], which utilize transfer learning and meta-learning techniques to adapt to target domains.

LLM-based Approaches: This category assesses the effectiveness of LLM-based strategies, comprising both fine-tuned and parameter-frozen approaches. LogLLM first encodes log sequences into feature vectors and then performs efficient supervised fine-tuning of the LLM for anomaly detection. Among the frozen models, LogPrompt utilizes zero-shot prompting, relying solely on the LLM's intrinsic knowledge. LogRAG [40] is a hybrid unsupervised method combining a DeepSVDD classifier with Retrieval-Augmented Generation (RAG) technology [41]. To assess the efficacy of off-the-shelf ICL strategies in the log text domain, we adapt two standard baselines widely used in general NLP tasks [42], [43]. Random-ICL selects demonstrations via uniform random sampling from the candidate pool, serving as a stochastic baseline to measure the impact of demonstration content. k NN-ICL retrieves the top- k nearest neighbors based on cosine similarity in the embedding space, representing a standard retrieval-augmented approach without domain-specific optimization.

5) *Evaluation Metrics*: We choose Precision, Recall, and F1-Score as the evaluation measurements, with the defini-

TABLE II
EVALUATION UNDER CROSS-DOMAIN FEW-SHOT SETTINGS (PRECISION, RECALL, F1-SCORE).

Method	Type	Liberty-BGL			BGL-TB			BGL-Liberty			TB-Liberty		
		P(%)	R(%)	F1(%)	P(%)	R(%)	F1(%)	P(%)	R(%)	F1(%)	P(%)	R(%)	F1(%)
LogRobust	Supervised	39.01	87.06	53.88	4.78	0.01	0.03	6.99	0.12	0.23	54.66	2.53	4.83
LogTransfer	Supervised Cross-System	0.00	0.00	0.00	33.84	100.00	50.57	0.00	0.00	0.00	0.00	0.00	0.00
LogTAD	Unsupervised Cross-System	62.60	58.33	59.91	60.77	61.10	60.87	86.49	66.24	66.95	84.41	67.50	68.63
MetaLog	Supervised Cross-System	65.78	59.09	62.26	47.03	99.87	63.94	35.02	54.33	42.59	80.98	89.58	85.06
LogLLM	LLM-based (fine-tune)	40.55	11.13	17.47	70.87	37.94	49.43	59.09	99.91	74.26	-	-	-
LogPrompt	LLM-based (frozen)	39.35	76.61	52.00	51.12	70.65	59.32	66.62	47.30	55.32	-	-	-
LogRAG	Unsupervised & LLM (frozen)	91.00	98.56	29.13	44.66	100.00	61.74	88.40	100.00	93.84	-	-	-
Random-ICL	LLM-based (frozen)	29.96	100.00	34.65	30.82	100.00	47.12	66.26	100.00	79.71	65.53	96.44	78.04
<i>k</i> NN-ICL	LLM-based (frozen)	29.31	31.28	30.26	40.13	37.85	38.95	33.80	6.62	11.07	90.58	53.77	67.48
LogICL (Ours)	LLM-based (frozen)	70.29	78.21	74.04	91.16	87.54	89.32	74.44	85.43	79.56	81.83	88.87	85.20

TABLE III
EVALUATION UNDER CROSS-DOMAIN ZERO-SHOT SETTINGS (PRECISION, RECALL, F1-SCORE).

Method	Type	BGL-Liberty-TB			Liberty-BGL-TB			TB-Liberty-BGL			BGL-TB-Liberty			TB-Liberty-HDFS		
		P(%)	R(%)	F1(%)	P(%)	R(%)	F1(%)									
LogRobust	Supervised	57.36	91.79	70.60	18.07	4.59	7.32	66.48	31.69	42.92	79.15	5.29	9.91	2.43	82.50	4.73
LogPrompt	LLM-based (frozen)	51.12	70.65	59.32	-	-	-	39.35	76.61	52.00	66.62	47.30	55.32	8.73	84.07	15.81
MetaLog	Supervised Cross-System	42.10	86.23	56.58	56.70	73.50	64.01	29.16	23.35	25.93	90.72	10.02	18.04	3.50	0.50	0.10
LogICL (Ours)	LLM-based (frozen)	70.16	79.83	74.68	65.96	66.06	66.01	40.21	34.71	37.25	82.39	69.70	75.52	72.87	22.57	34.68

tions of $Precision = \frac{TP}{TP+FP}$, $Recall = \frac{TP}{TP+FN}$, and $F1 = \frac{2 \cdot Precision \cdot Recall}{Precision + Recall}$. Here, TP , FP , and FN denote the number of true positives, false positives, and false negatives, respectively.

6) *Implementation Details*: We implement our framework in PyTorch with Python 3.11, accelerated by two NVIDIA H200 GPUs (141 GB). We employ Sentence-BERT as the backbone encoder. It maps log sequence to a 384-dimensional dense vector space, while Qwen3-14B [44] serves as the core LLM, deployed via vLLM. In the training phase, we iterate through each training sample as a query and employ MMR to retrieve 128 candidates for constructing the delta matrix. In the test phase, we retrieve 8 demonstrations for each test query to perform inference. The weighting coefficients for the multi-objective loss are empirically set to $\lambda_{MMD} = 0.1$, $\lambda_{SupCon} = 1.0$, and $\lambda_{Delta} = 1.0$. Consistent with standard practices, we apply a classification threshold of 0.5 to determine anomaly labels. **Our code is open-sourced in <https://zenodo.org/records/17850648>**

B. Evaluation under Cross-Domain Few-Shot Settings

To comprehensively evaluate the effectiveness of our proposed framework, we compare LogICL with a wide range of baselines. Table II presents the comparative results in terms of Precision, Recall, and F1-Score across four cross-domain scenarios.

1) *Baselines and Experimental Configurations*: It is important to clarify the specific experimental configurations adopted

to ensure a fair and realistic comparison, particularly where they deviate from the original papers:

For LogRobust, we adjusted its original fully supervised setting (using an 8:2 split for training and testing) to align with our cross-domain few-shot setting. It was trained on 50,000 source domain samples and adapted using 5,000 target domain samples.

For LogTransfer and LogTAD, we employ the same source and target domain splits as LogICL. The training and testing sample quantities are kept strictly consistent across all experiments to ensure a fair comparison.

For LogLLM, LogPrompt, and LogRAG, since their original architectures do not inherently support cross-domain transfer mechanisms, we followed their respective intra-domain settings using the 5,000 target domain samples for training. As a result, the experimental setup for TB-Liberty becomes identical to BGL-Liberty (both relying solely on the Liberty target data); thus, we omit redundant results for TB-Liberty (marked as “-”).

For Random-ICL and *k*NN-ICL, we construct a shared demonstration pool comprising 50,000 labeled source-domain samples and 5,000 labeled target-domain samples. During inference, demonstrations are retrieved from this pool via random sampling or *k*-nearest neighbor matching in the embedding space, respectively, and are provided alongside the test query to the LLM for anomaly prediction.

2) *Comparative Analysis and Discussion*: The results in Table II provide key insights into the performance of baselines

under cross-domain few-shot log anomaly detection. Traditional supervised and transfer learning methods show limited generalization. LogRobust, as a supervised model, requires ample labeled data for training and exhibits sharp declines in cross-domain scenarios (e.g., F1 of 0.03% on BGL-TB), due to inadequate adaptation with sparse target supervision. LogTransfer, a supervised cross-system approach, is highly sensitive to data distributions; in our chronological split with only 5,000 target samples (below the 300 anomalies needed for effective transfer, as reported in the original work), it often defaults to classifying all logs as normal, yielding 0.00% F1 in three out of four transfers (Liberty-BGL, BGL-Liberty, TB-Liberty). LogTAD and MetaLog fare better in some cases but remain inconsistent, as their reliance on pre-trained word embeddings for feature extraction captures only surface lexical similarity, overlooking latent semantic equivalence amid structural and terminological differences, which degrades accuracy under limited target data (e.g., MetaLog’s 42.59% F1 on BGL-Liberty). LLM-based methods demonstrate greater potential but encounter specific limitations. LogLLM, which involves fine-tuning, needs extensive data to harness its large parameters for robust generalization, leading to low scores with scarce target labels (e.g., 17.47% F1 on Liberty-BGL). LogPrompt, using frozen LLMs, achieves moderate results but struggles without optimized prompts and demonstrations to activate the model’s prior knowledge for precise log anomaly detection (e.g., 55.32% F1 on BGL-Liberty). LogRAG combines unsupervised retrieval-augmented generation with a deepSVDD classifier, which demands sufficient training data; in data-scarce settings, poor retrieval of beneficial contexts causes instability (e.g., 29.13% F1 on Liberty-BGL despite 93.84% on BGL-Liberty). The ICL baselines, Random-ICL and k NN-ICL, generally underperform because random or embedding-based selection often yields irrelevant or interfering demonstrations, failing to improve downstream anomaly prediction (e.g., k NN-ICL’s 11.07% F1 on BGL-Liberty).

3) *Effectiveness of LogICL*: In contrast, LogICL achieves state-of-the-art F1 scores in three transfers (74.04% on Liberty-BGL, 89.32% on BGL-TB, 85.20% on TB-Liberty) and remains competitive in the fourth (79.56% on BGL-Liberty), outperforming baselines by distilling LLM reasoning into the encoder and retrieving high-utility demonstrations. This mechanism effectively captures latent semantic equivalence, bridging domain gaps without fine-tuning or abundant target data.

C. Evaluation under Cross-Domain Zero-Shot Settings

In this section, we impose a stricter zero-shot evaluation setting, where the model must generalize to a completely unseen target domain. Table III shows the performance of LogICL compared against supervised baselines (LogRobust, MetaLog) and an LLM-based inference baseline (LogPrompt).

1) *Baselines and Experimental Configurations*: The supervised baselines, LogRobust and MetaLog, are trained on a composite dataset comprising 50,000 samples from the primary source and 5,000 from the auxiliary source, and then evaluated on the unseen target domain. In contrast, LogPrompt

operates with frozen parameters, bypassing the training phase to perform zero-shot inference directly via prompting. Since LogPrompt’s performance depends solely on the target domain and is independent of source data configurations, we mark redundant entries with “-” to avoid repetition.

2) *Comparative Analysis and Discussion*: The results in Table III highlight the generalization limitations of existing supervised and meta-learning approaches. LogRobust, which relies on static semantic embeddings and a supervised classifier, depends heavily on labeled target-domain data and suffers from severe overfitting when syntactic differences are pronounced (e.g., F1 drops to 4.73% on TB-Liberty-HDFS). Similarly, MetaLog uses meta-learning for task adaptation but requires a small support set of target labels; in a strict zero-shot setting, the absence of such cues leads to near-complete failure (e.g., 0.10% F1). Prompt-based methods show greater robustness by exploiting the broad semantic knowledge of LLMs. LogPrompt, in particular, delivers stable performance across most transfers and even surpasses LogICL on TB-Liberty-BGL (52.00% vs. 37.25% F1). However, without targeted demonstration retrieval, it struggles with fine-grained anomaly patterns in structurally complex datasets like HDFS (15.81% F1), limiting its effectiveness in highly heterogeneous environments. In contrast, LogICL consistently outperforms these baselines by distilling LLM reasoning guidance into the encoder and retrieving reasoning-aware demonstrations, enabling effective cross-domain transfer without any target-domain supervision. It is worth noting that the TB-Liberty-HDFS transfer represents the most challenging cross-domain scenario in our evaluation, bridging logs from a supercomputing environment to a distributed storage system. Compared to the first four transfers (all within supercomputing systems), the substantial differences in log structure, terminology, and failure modes reduce the amount of transferable knowledge from the source domain. This increased domain gap explains the overall lower performance on this transfer across all methods, underscoring the difficulty of achieving robust generalization in truly heterogeneous settings.

3) *Effectiveness of LogICL*: LogICL outperforms baselines in four out of five zero-shot scenarios, demonstrating superior generalization capabilities. Most notably, in the challenging TB-Liberty-HDFS setting, LogICL achieves an F1-score of 34.68%, which is more than double that of LogPrompt and significantly higher than the collapsed supervised methods. This indicates that even without target domain training, LogICL effectively utilizes latent semantic alignment demos retrieved from the source domains (TB and Liberty) to guide the LLM’s reasoning on the unseen target (HDFS). This capability to bridge the semantic gap via retrieval-augmented in-context learning is the key factor differentiating LogICL from traditional supervised, cross-system or static prompting approaches.

D. Parameter Sensitivity Analysis

In this section, we investigate the sensitivity of LogICL to the number of demonstrations (k). we constructed a randomized test set by shuffling the target domain data and sampling

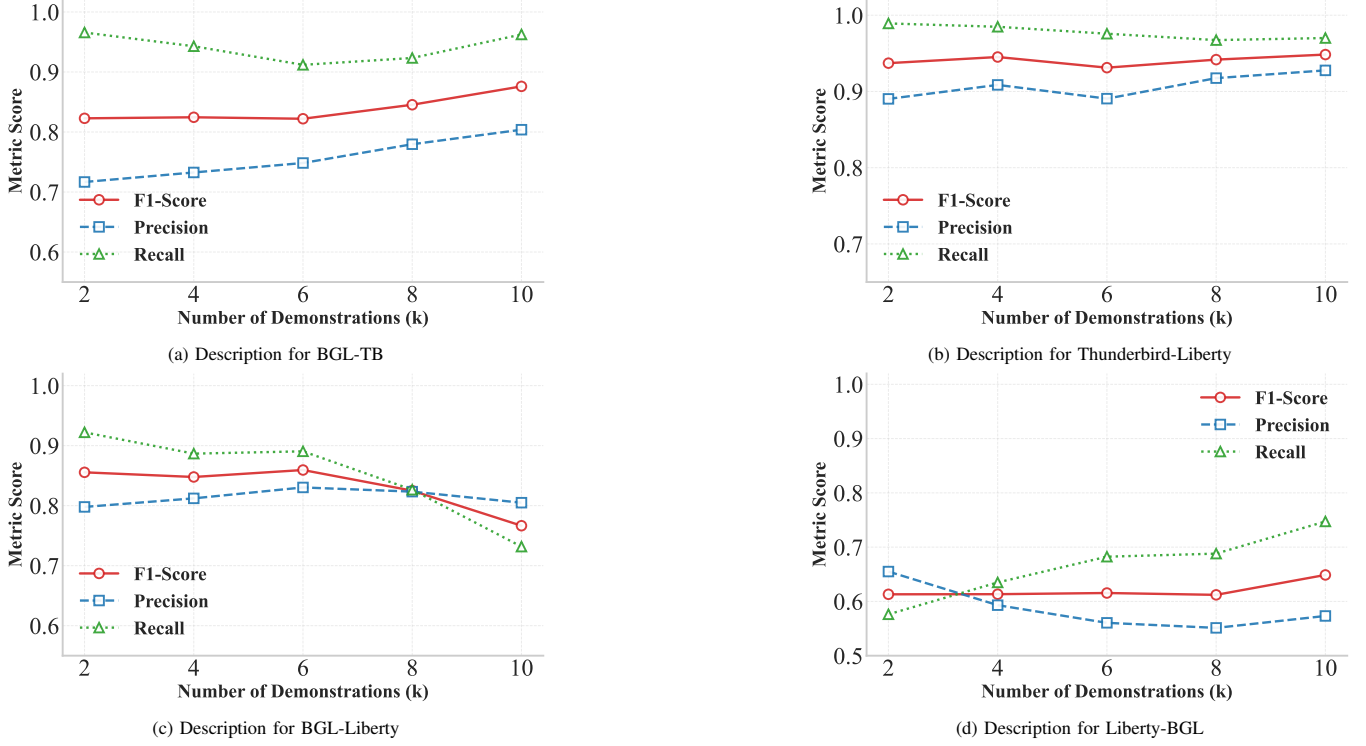


Fig. 6. Parameter sensitivity analysis across four different metrics.

5,000 instances. The number of retrieved demonstrations k , is varied within the range $\{2, 4, 6, 8, 10\}$, the decision threshold was fixed at $\tau = 0.5$. Figure 6 illustrates the trends of Precision, Recall, and F1-Score across four transfer scenarios.

As observed in Figure 6, the model’s overall performance generally exhibits an upward trend as k increases. For example, in the Liberty-BGL scenario (Figure 6(d)), the F1-score steadily improves as k rises from 2 to 10. This trend suggests that increasing the number of retrieved demonstrations enriches the context with a diverse spectrum of anomaly patterns from the source domain. This comprehensive reference information enables the LLM to better bridge the semantic gap, effectively transferring prior knowledge to distinguish anomalous behaviors in the target domain.

However, the performance improvement is not strictly monotonic. We observe declines in specific configurations (e.g., the Recall drop in the BGL-Liberty scenario when $k > 6$, as shown in Figure 6(c)). This phenomenon suggests that simply increasing the quantity of demonstrations does not always guarantee better inference; excessive demonstrations may introduce irrelevant noise or redundant patterns that interfere with the LLM’s reasoning process. Despite these minor fluctuations, LogICL maintains a high level of performance stability across varying k , demonstrating strong robustness to hyperparameter changes in few-shot settings.

E. Ablation Study

To verify the contribution of each proposed component, we conduct comprehensive ablation studies on the multi-objective optimization and the ICL-Guided Loss, with results reported

TABLE IV
ABLATION STUDY ON LOSS COMPONENTS.

Transfer Task	F1-Score (%)		
	w/o Opt	w/o ICL-Guided	LogICL
Liberty-BGL	23.73	38.11	74.04
BGL-Thunderbird	39.58	79.56	89.32
BGL-Liberty	59.35	73.49	79.56
Thunderbird-Liberty	71.95	83.65	85.20

in Table IV. We compare the complete LogICL framework against two ablated variants: (1) *w/o Opt*, which freezes the log encoder and relies solely on the raw pre-trained representation without any optimization, and (2) *w/o ICL-Guided*, which removes only the L_{Δ} component while retaining the other training objectives.

As shown in Table IV, the *w/o Opt* variant exhibits dramatically lower performance across all transfer tasks, achieving only 23.73% F1 on Liberty-BGL—the most challenging cross-system transfer—and at most 71.95% F1 on the relatively easier Thunderbird-Liberty transfer. This sharp degradation underscores that a frozen encoder, even when pre-trained on massive log data, cannot effectively bridge the substantial domain gap between different logging systems without explicit alignment and task-adaptive fine-tuning.

Removing only the ICL-Guided Loss (*w/o ICL-Guided*) yields substantial gains over the frozen baseline (e.g., +14.38 points on Liberty-BGL and +39.98 points on BGL-Thunderbird), demonstrating the benefit of basic contrastive domain adaptation. Nevertheless, this variant still lags consid-

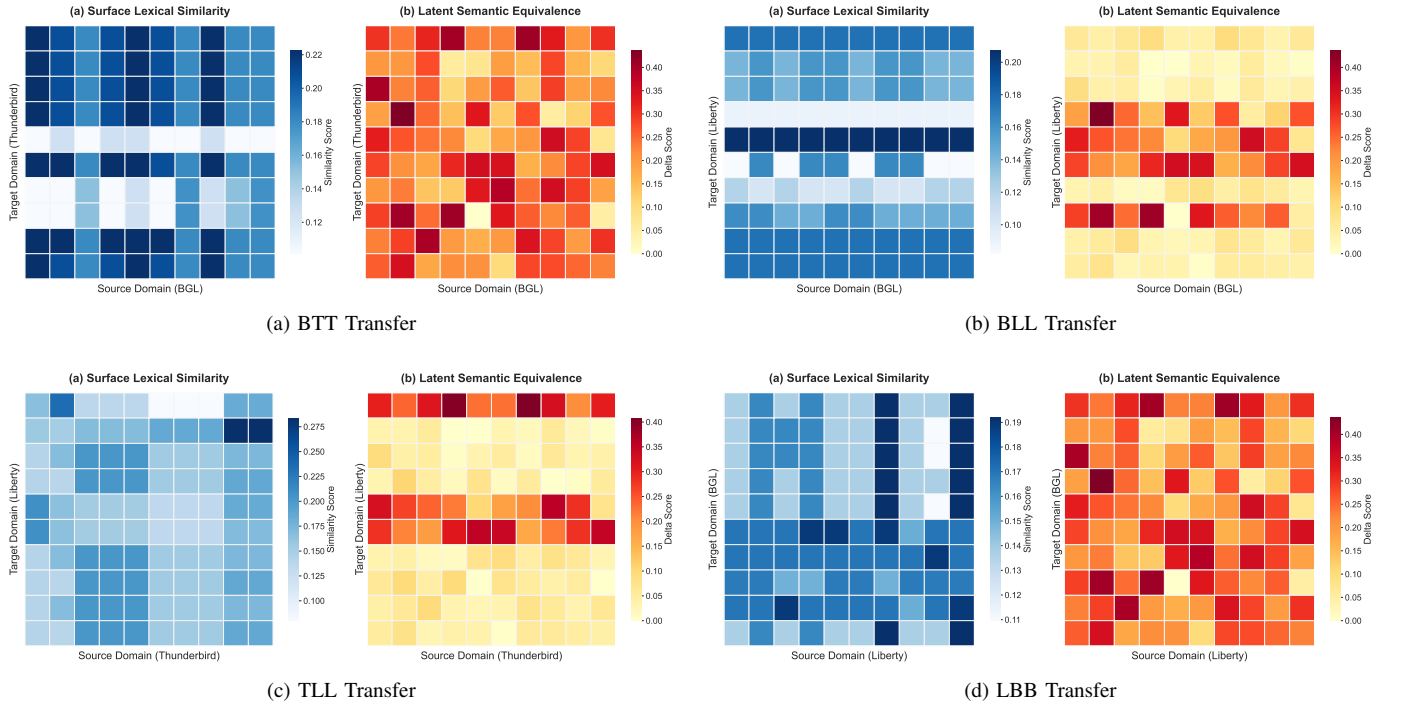


Fig. 7. **Visualization of Alignment Mechanisms.** Comparison between surface lexical similarity (blue, left) and Latent Semantic Equivalence (red, right) across (a) BTT, (b) BLL, (c) TLL, and (d) LBB scenarios. The contrast highlights LogICL’s ability to overcome vocabulary mismatches by capturing deep **semantic equivalence** and **structural homology** (e.g., matching error burst patterns), confirming that demonstrations serve as effective structural prototypes.

erably behind the full LogICL model, with gaps ranging from 11.55 to 35.93 F1 points across tasks. The most pronounced drop occurs on the Liberty-BGL transfer (38.11% vs. 74.04%), highlighting that, without the explicit supervision from L_{Δ} , the encoder tends to capture superficial lexical patterns or source-system biases rather than the deeper semantic invariants that the LLM actually leverages during in-context reasoning.

The full LogICL framework, which jointly optimizes all objectives, consistently achieves the highest performance, reaching 74.04%–89.32% F1 across diverse cross-system transfers. These results conclusively validate that both trainable domain-adaptive optimization and the ICL-Guided semantic alignment signal are indispensable for narrowing the modality and distribution gap between structured log representations and the LLM’s in-context learning mechanism. The synergistic integration of these components is the key to robust and generalizable cross-system log anomaly detection.

F. Interpretability of Alignment Mechanisms

To empirically validate the interpretability of LogICL, we visualize the alignment mechanisms across four cross-domain scenarios. As illustrated in Figure 7, in these heatmaps, the x-axis represents samples from the source domain, and the y-axis represents samples from the target domain. Each cell quantifies the pairwise relationship between a source-target pair using two distinct metrics: Surface Lexical Similarity (Blue Matrices, calculated via cosine similarity) and Latent Semantic Equivalence (Red Matrices, it is also the delta matrix).

1) *Lexical Disparity (Blue Matrices):* As shown in the blue heatmaps, the overall color distribution is predominantly light,

indicating consistently low cosine similarity scores across most cross-domain pairs. This visual evidence confirms a severe lexical disparity: the distinct system environments (e.g., BGL vs. Liberty) share negligible vocabulary overlap, rendering traditional keyword-based retrieval methods ineffective as they fail to find relevant neighbors in the source domain.

2) *Semantic Equivalence (Red Matrices):* In contrast, the red heatmaps exhibit distinct clusters of dark red regions (high delta scores). These “hot spots” indicate that despite the low lexical similarity, specific source demonstrations make significant contributions to the model’s reasoning process. This discrepancy captures deep semantic equivalence, where LogICL successfully identifies source logs that are textually distinct but functionally analogous to the target logs. The retrieved demonstrations act as structural prototypes, guiding the LLM to perform robust inductive reasoning beyond superficial keyword matching.

G. Case study

To validate the effectiveness of our delta-guided retrieval mechanism, we analyze a representative high-delta pair identified during inference. This pair shows minimal lexical overlap ($similarity < 0.1$) yet provides a strong positive contribution to detection accuracy ($\delta > 0.8$). As illustrated in Table V, the target domain sequence BGL contains repeated *generating core* events indicating persistent process crashes, while the retrieved demonstration from the Thunderbird consists mainly of *dhcpc: no free leases* errors. Despite their distinct vocabularies, the model establishes meaningful semantic alignment and structural correspondence between the two domains. Semantically, both sequences describe a form of *Resource*

TABLE V
QUALITATIVE ANALYSIS: BRIDGING SURFACE LEXICAL GAPS VIA LATENT SEMANTIC ALIGNMENT.

Role	Log Sequence Context	Surface Semantics	Latent Alignment
Target Domain (BGL)	generating core.2516 ;-; generating core.2517 ;-; generating core.2380 ;-; generating core.2382 ;-; generating core.2509 ...	Process Crash (Memory Context)	Mechanism: 1. Resource Exhaustion (Availability Collapse)
Retrieved Demo (Thunderbird)	dhcpd: DHCPDISCOVER from ... network 172.30.0/16: no free leases ;-; dhcpd: DHCPDISCOVER from ... network 172.31.0/16: no free leases ...	Alloc. Failure (Network Context)	2. Burstiness Pattern (High-Freq Repetition)

Exhaustion: the target reflects system context failure, and the source reflects address pool depletion. Structurally, the demonstration illustrates a typical *Burstiness Pattern* (high-frequency repetition indicates a system infinite loop or a retry storm), allowing the model to learn through in-context examples that frequent repetition of a critical error signals a system-level anomaly. This case indicates that our multi-objective loss encourages the model to move beyond keyword matching and supports robust reasoning across heterogeneous system environments.

H. Threats to Validity

We acknowledge three primary factors that may impact the validity and generalization of our findings.

Sensitivity to Prompt Design. The inference accuracy of ICL is contingent upon the quality of instruction templates. As instructional ambiguity can act as a confounding variable, suboptimal prompt engineering may potentially mask the performance gains attributed to our demonstration retrieval mechanism.

Gap between Frozen LLMs and Domain Expertise. While LogICL effectively bridges semantic gaps via context, general-purpose LLMs lack intrinsic AIOps expertise. Since our approach operates without parameter updates, the model’s deductive reasoning is bounded by its pre-trained knowledge. Achieving human-level reliability in complex diagnostics may necessitate integrating explicit domain adaptation strategies, such as Reinforcement Learning from Human Feedback (RLHF).

Impact of Model Scale. Foundational research [19] characterizes the capacity for in-context learning in few-shot tasks as an emergent ability that scales significantly with model size. Our deployment of a moderate-sized model (14B)—chosen to balance computational efficiency—may not fully unlock the peak reasoning potential observed in larger foundation models (e.g., 175B), representing a necessary trade-off between resource constraints and optimal few-shot performance.

V. DISCUSSION

Beyond Metrics: Reality Check on Anomaly Discovery. Our initial experiments on the BGL dataset exhibited an unusually high False Positive Rate compared to other benchmarks, prompting a deeper investigation into these “misclassifications.” Upon manual inspection, we discovered that these

instances were largely latent anomalies mislabeled as normal in the ground truth. This phenomenon highlights a critical distinction in model behavior: while traditional supervised baselines tend to overfit label noise within the closed-world training data—yielding superficially high metrics—LogICL exposes these inconsistencies. This capability stems from the frozen LLM’s extensive pre-trained world knowledge, which acts as an external “knowledge auditor”. By leveraging intrinsic semantic understanding of system failures, LogICL identifies anomaly patterns that contradict erroneous labels. To address this rigorously, we corrected the BGL dataset following the Expert-Driven Data Correction setting established by a prior study [28]. We have integrated this label rectification pipeline into our open-source code to facilitate reproducibility and encourage future research to prioritize dataset reliability over raw metric inflation.

VI. CONCLUSION

In this paper, we proposed LogICL, a novel cross-domain framework designed to address the cold-start challenge in log anomaly detection by bridging the gap between surface lexical similarity and latent semantic equivalence. Unlike traditional transfer learning methods constrained by static embeddings or data-intensive Transformer adaptations, LogICL distills the reasoning capabilities of LLMs into a lightweight encoder via a novel delta matrix and multi-objective optimization. This approach enables the retrieval of reasoning-aware demonstrations that facilitate effective ICL with a frozen LLM. Extensive experiments on cross-system benchmarks demonstrate that LogICL achieves state-of-the-art performance in both few-shot and zero-shot settings, outperforming existing baselines. By combining robust generalization with Chain-of-Thought traceability for enhanced diagnostic insights, LogICL offers a resource-efficient solution for rapid deployment in evolving IT infrastructures.

REFERENCES

- [1] S. He, P. He, Z. Chen, T. Yang, Y. Su, and M. R. Lyu, “A survey on automated log analysis for reliability engineering,” *ACM computing surveys (CSUR)*, vol. 54, no. 6, pp. 1–37, 2021.
- [2] S. He, J. Zhu, P. He, and M. R. Lyu, “Experience report: System log analysis for anomaly detection,” in *2016 IEEE 27th international symposium on software reliability engineering (ISSRE)*. IEEE, 2016, pp. 207–218.
- [3] H. Guo, S. Yuan, and X. Wu, “Logbert: Log anomaly detection via bert,” in *2021 international joint conference on neural networks (IJCNN)*. IEEE, 2021, pp. 1–8.

[4] Z. Chen, Q. Gao, and L. S. Moss, “Neurallog: Natural language inference with joint neural and logical reasoning,” *arXiv preprint arXiv:2105.14167*, 2021.

[5] J. Ye, C. Liu, Z. Gu, Z. Zhang, X. Meng, W. Zhang, and Y. Zhang, “Logow: A semi-supervised log anomaly detection model in open-world setting,” *Journal of Systems and Software*, vol. 222, p. 112305, 2025.

[6] X. Han, S. Yuan, and M. Trabelsi, “Logppt: Log anomaly detection via gpt,” in *2023 IEEE International Conference on Big Data (BigData)*. IEEE, 2023, pp. 1117–1122.

[7] W. Guan, J. Cao, S. Qian, J. Gao, and C. Ouyang, “Loglm: Log-based anomaly detection using large language models,” *arXiv preprint arXiv:2411.08561*, 2024.

[8] L. Torrey and J. Shavlik, “Transfer learning,” in *Handbook of research on machine learning applications and trends: algorithms, methods, and techniques*. IGI Global Scientific Publishing, 2010, pp. 242–264.

[9] R. Chen, S. Zhang, D. Li, Y. Zhang, F. Guo, W. Meng, D. Pei, Y. Zhang, X. Chen, and Y. Liu, “Logtransfer: Cross-system log anomaly detection for software systems with transfer learning,” in *2020 IEEE 31st International Symposium on Software Reliability Engineering (ISSRE)*. IEEE, 2020, pp. 37–47.

[10] X. Han and S. Yuan, “Unsupervised cross-system log anomaly detection via domain adaptation,” in *Proceedings of the 30th ACM international conference on information & knowledge management*, 2021, pp. 3068–3072.

[11] C. Zhang, T. Jia, G. Shen, P. Zhu, and Y. Li, “Metalog: Generalizable cross-system anomaly detection from logs with meta-learning,” in *Proceedings of the IEEE/ACM 46th International Conference on Software Engineering*, 2024, pp. 1–12.

[12] J. Pennington, R. Socher, and C. D. Manning, “Glove: Global vectors for word representation,” in *Proceedings of the 2014 conference on empirical methods in natural language processing (EMNLP)*, 2014, pp. 1532–1543.

[13] E. J. Hu, Y. Shen, P. Wallis, Z. Allen-Zhu, Y. Li, S. Wang, L. Wang, W. Chen *et al.*, “Lora: Low-rank adaptation of large language models.” *ICLR*, vol. 1, no. 2, p. 3, 2022.

[14] K. Weiss, T. M. Khoshgoftaar, and D. Wang, “A survey of transfer learning,” *Journal of Big data*, vol. 3, no. 1, p. 9, 2016.

[15] F. Zhuang, Z. Qi, K. Duan, D. Xi, Y. Zhu, H. Zhu, H. Xiong, and Q. He, “A comprehensive survey on transfer learning,” *Proceedings of the IEEE*, vol. 109, no. 1, pp. 43–76, 2020.

[16] S. J. Pan and Q. Yang, “A survey on transfer learning,” *IEEE Trans. Knowl. Data Eng.*, vol. 22, no. 10, pp. 1345–1359, 2010. [Online]. Available: <https://doi.org/10.1109/TKDE.2009.191>

[17] Q. Dong, L. Li, D. Dai, C. Zheng, J. Ma, R. Li, H. Xia, J. Xu, Z. Wu, T. Liu *et al.*, “A survey on in-context learning,” *arXiv preprint arXiv:2301.00234*, 2022.

[18] J. Pan, T. Gao, H. Chen, and D. Chen, “What in-context learning “learns” in-context: Disentangling task recognition and task learning,” in *Findings of the Association for Computational Linguistics: ACL 2023*, 2023, pp. 8298–8319.

[19] T. Brown, B. Mann, N. Ryder, M. Subbiah, J. D. Kaplan, P. Dhariwal, A. Neelakantan, P. Shyam, G. Sastry, A. Askell *et al.*, “Language models are few-shot learners,” *Advances in neural information processing systems*, vol. 33, pp. 1877–1901, 2020.

[20] J. Von Oswald, E. Niklasson, E. Randazzo, J. Sacramento, A. Mordvintsev, A. Zhmoginov, and M. Vladymyrov, “Transformers learn in-context by gradient descent,” in *International Conference on Machine Learning*. PMLR, 2023, pp. 3515–35174.

[21] S. M. Xie, A. Raghunathan, P. Liang, and T. Ma, “An explanation of in-context learning as implicit bayesian inference,” *arXiv preprint arXiv:2111.02080*, 2021.

[22] F. Falck, Z. Wang, and C. Holmes, “Is in-context learning in large language models bayesian? a martingale perspective,” *arXiv preprint arXiv:2406.00793*, 2024.

[23] Z. Ma, A. R. Chen, D. J. Kim, T.-H. Chen, and S. Wang, “Llmparser: An exploratory study on using large language models for log parsing,” in *Proceedings of the IEEE/ACM 46th International Conference on Software Engineering*, 2024, pp. 1–13.

[24] X. Huang, T. Zhang, and W. Zhao, “Logrules: Enhancing log analysis capability of large language models through rules,” in *Findings of the Association for Computational Linguistics: NAACL 2025*, 2025, pp. 452–470.

[25] F. Hadadi, Q. Xu, D. Bianculli, and L. Briand, “Llm meets ml: Data-efficient anomaly detection on unstable logs,” *ACM Transactions on Software Engineering and Methodology*, 2025.

[26] C. Duan, T. Jia, Y. Yang, G. Liu, J. Liu, H. Zhang, Q. Zhou, Y. Li, and G. Huang, “Eagerlog: Active learning enhanced retrieval augmented generation for log-based anomaly detection,” in *ICASSP 2025-2025 IEEE International Conference on Acoustics, Speech and Signal Processing (ICASSP)*. IEEE, 2025, pp. 1–5.

[27] Y. Ji, Y. Liu, F. Yao, M. He, S. Tao, X. Zhao, S. Chang, X. Yang, W. Meng, Y. Xie *et al.*, “Adapting large language models to log analysis with interpretable domain knowledge,” *arXiv preprint arXiv:2412.01377*, 2024.

[28] S. Xu, Y. Liu, M. He, M. Dai, Z. Chen, C. Zhao, J. Du, S. Tao, W. Meng, S. Zhang *et al.*, “Rationanomaly: Log anomaly detection with rationality via chain-of-thought and reinforcement learning,” *arXiv preprint arXiv:2509.14693*, 2025.

[29] A. Gretton, K. M. Borgwardt, M. J. Rasch, B. Schölkopf, and A. Smola, “A kernel two-sample test,” *The journal of machine learning research*, vol. 13, no. 1, pp. 723–773, 2012.

[30] P. He, J. Zhu, Z. Zheng, and M. R. Lyu, “Drain: An online log parsing approach with fixed depth tree,” in *2017 IEEE international conference on web services (ICWS)*. IEEE, 2017, pp. 33–40.

[31] Z. Jiang, J. Liu, J. Huang, Y. Li, Y. Huo, J. Gu, Z. Chen, J. Zhu, and M. R. Lyu, “A large-scale evaluation for log parsing techniques: How far are we?” in *Proceedings of the 33rd ACM SIGSOFT International Symposium on Software Testing and Analysis*, 2024, pp. 223–234.

[32] Z. Jiang, J. Liu, Z. Chen, Y. Li, J. Huang, Y. Huo, P. He, J. Gu, and M. R. Lyu, “Lilac: Log parsing using llms with adaptive parsing cache,” *Proceedings of the ACM on Software Engineering*, vol. 1, no. FSE, pp. 137–160, 2024.

[33] V.-H. Le and H. Zhang, “Log parsing with prompt-based few-shot learning,” in *2023 ieee/acm 45th international conference on software engineering (icse)*, Los Alamitos, CA, USA. IEEE Computer Society, pp. 2438–2449, 2023.

[34] J. Carbonell and J. Goldstein, “The use of mmr, diversity-based reranking for reordering documents and producing summaries,” in *Proceedings of the 21st annual international ACM SIGIR conference on Research and development in information retrieval*, 1998, pp. 335–336.

[35] B. K. Sriperumbudur, A. Gretton, K. Fukumizu, B. Schölkopf, and G. R. Lanckriet, “Hilbert space embeddings and metrics on probability measures,” *The Journal of Machine Learning Research*, vol. 11, pp. 1517–1561, 2010.

[36] P. Khosla, P. Teterwak, C. Wang, A. Sarna, Y. Tian, P. Isola, A. Maschinot, C. Liu, and D. Krishnan, “Supervised contrastive learning,” *Advances in neural information processing systems*, vol. 33, pp. 18661–18673, 2020.

[37] A. Oliner and J. Stearley, “What supercomputers say: A study of five system logs,” in *37th annual IEEE/IFIP international conference on dependable systems and networks (DSN’07)*. IEEE, 2007, pp. 575–584.

[38] W. Xu, L. Huang, A. Fox, D. Patterson, and M. I. Jordan, “Detecting large-scale system problems by mining console logs,” in *Proceedings of the ACM SIGOPS 22nd symposium on Operating systems principles*, 2009, pp. 117–132.

[39] X. Zhang, Y. Xu, Q. Lin, B. Qiao, H. Zhang, Y. Dang, C. Xie, X. Yang, Q. Cheng, Z. Li *et al.*, “Robust log-based anomaly detection on unstable log data,” in *Proceedings of the 2019 27th ACM joint meeting on European software engineering conference and symposium on the foundations of software engineering*, 2019, pp. 807–817.

[40] W. Zhang, Q. Zhang, E. Yu, Y. Ren, Y. Meng, M. Qiu, and J. Wang, “Lograg: Semi-supervised log-based anomaly detection with retrieval-augmented generation,” in *2024 IEEE International Conference on Web Services (ICWS)*. IEEE, 2024, pp. 1100–1102.

[41] P. Lewis, E. Perez, A. Piktus, F. Petroni, V. Karpukhin, N. Goyal, H. Küttler, M. Lewis, W.-t. Yih, T. Rocktäschel *et al.*, “Retrieval-augmented generation for knowledge-intensive nlp tasks,” *Advances in neural information processing systems*, vol. 33, pp. 9459–9474, 2020.

[42] C. Qin, A. Zhang, C. Chen, A. Dagar, and W. Ye, “In-context learning with iterative demonstration selection,” in *Findings of the Association for Computational Linguistics: EMNLP 2024*, 2024, pp. 7441–7455.

[43] K. Peng, L. Ding, Y. Yuan, X. Liu, M. Zhang, Y. Ouyang, and D. Tao, “Revisiting demonstration selection strategies in in-context learning,” *arXiv preprint arXiv:2401.12087*, 2024.

[44] A. Yang, A. Li, B. Yang, B. Zhang, B. Hui, B. Zheng, B. Yu, C. Gao, C. Huang, C. Lv *et al.*, “Qwen3 technical report,” *arXiv preprint arXiv:2505.09388*, 2025.